Logic-based machine learning predicts how escitalopram inhibits cardiomyocyte hypertrophy

Taylor G. Eggertsen, Joshua G. Travers, Elizabeth J. Hardy, Matthew J. Wolf, Timothy A. McKinsey, and Jeffrey J. Saucerman

Contact: jsaucerman@virginia.edu

ABSTRACT

Introduction

Cardiomyocyte hypertrophy is a key clinical predictor of heart failure. High-throughput and AI-driven screens have potential to identify drugs and downstream pathways that modulate cardiomyocyte hypertrophy.

Methods

Here we developed LogiRx, a logic-based mechanistic machine learning method that predicts drug-induced pathways. We applied LogiRx to discover how drugs discovered in a previous compound screen attenuate cardiomyocyte hypertrophy. We experimentally validated LogiRx predictions in neonatal cardiomyocytes, adult mice, and two patient databases.

Results

Using LogiRx, we predicted anti-hypertrophic pathways for 7 drugs currently used to treat non-cardiac disease. We experimentally validated that escitalopram (Lexapro) and mifepristone inhibit hypertrophy of cultured cardiomyocytes in two contexts. The LogiRx model predicted that escitalopram prevents hypertrophy through an "off-target" serotonin receptor/PI3Kγ pathway, mechanistically validated using additional investigational drugs. Further, escitalopram reduced cardiomyocyte hypertrophy in a mouse model of hypertrophy and fibrosis. Finally, mining of both FDA and University of Virginia databases showed that patients with depression on escitalopram have a lower incidence of cardiac hypertrophy than those prescribed other serotonin reuptake inhibitors that do not target the serotonin receptor.

Conclusion

Mechanistic machine learning by LogiRx discovers drug pathways that perturb cell states, which may enable repurposing of escitalopram and other drugs to limit cardiac remodeling through "off-target" pathways.

30 **INTRODUCTION**

31 Cardiac hypertrophy is a key clinical predictor of heart failure[1–5]. Hypertrophy is a response to
32 various physiological stressors, such as pressure overload, drug toxicity, or gene mutations[6]. Several
33 drugs prescribed for heart failure also affect cardiac hypertrophy, such as angiotensin converting
34 enzyme (ACE) inhibitors, beta blockers, and angiotensin receptor blockers (ARBs)[7]. But heart failure
35 rates are still rising, with a five year mortality rate > 40%[8]. There has been increasing effort towards drug
36 repurposing for cardiovascular indications to accelerate translation and reduce cost[9,10]. One such
37 success is the repurposing of SGLT2 inhibitors from diabetes to cardiovascular disease[11].

38 Numerous medications not initially designed for cardiac treatment impact the progression of
39 cardiac hypertrophy[12–15], although their mechanisms are largely unknown. Experimental approaches to
40 prioritize drugs from large screens and investigate their mechanisms are time intensive and costly. Drug
41 development is further hindered by the complexity of hypertrophic signaling, with a high degree of
42 cross-talk between multiple molecular pathways[7,16]. Protein interaction databases and gene regulatory
43 networks have been used previously to explore drug target interactions[17,18], however these studies have
44 primarily examined network topology rather than simulating network response to drugs.

45 To address the challenges of mapping and mechanistically understanding drug responses from
46 phenotypic screens, we developed a logic-based predictor of drug pathways (LogiRx). LogiRx maps from
47 drug-target and protein interaction databases to curated logic-based network models of cell phenotype.
48 We used LogiRx to prioritize seven anti-hypertrophic drugs identified in a previous cell-based screen[12],
49 providing mechanistic insight to how two drugs attenuate hypertrophy via “off-target” pathways. LogiRx
50 predictions were experimentally validated in cultured cardiomyocytes, mice, and in two patient
51 databases of electronic health records. Together, these studies validate the LogiRx method and provide
52 mechanistic insights into how escitalopram (Lexapro) and other drugs modulate cardiomyocyte
53 hypertrophy.

54

55 **METHODS**

56 **Logic-based network model**

57 We used a published logic-based differential equation model of the cardiomyocyte hypertrophy
58 signaling network[19]. Netflux software (bioRxiv 2024.01.11.575227) was used to construct the network
59 model from a literature-based network of proteins and genes previously associated with cardiomyocyte
60 hypertrophy. This network model is composed of 107 nodes (proteins or mRNAs) and 193 edges, with 17
61 biochemical inputs including a mechanical stretch input. Outputs include hypertrophic markers, beta
62 myosin heavy chain (βMHC), atrial natriuretic hormone (ANP), brain natriuretic peptide (BNP) and cell
63 area. As in previous studies, biochemical or stretch stimulation was simulated by setting input reaction
64 weights to a value of 0.1, representing 10% of saturating activity[20]. Examining 450 experiments across
65 the literature, this model had a 77% accuracy[20]. Further, the model correctly predicted the anti-
66 hypertrophic effect of 28 out of 32 drug responses from our previous experimental screen[12], further
67 examined by LogiRx below.

68 **Linking drug targets to logic-based signaling network using LogiRx**

69 LogiRx uses mechanistic machine learning to map pathways from drugs into a validated logic-
70 based network model. We first identified hits from a previous screen for compounds that inhibit
71 cardiomyocyte hypertrophy[12]. Protein targets for these active compounds were identified using the
72 drug-target database DrugBank[21] based on gene name. Directed protein interactions in the Omnipath
73 protein interaction database[22,23] originating from the KEGG[24], Reactome[25], and SIGNOR[26] datasets were
74 used as potential connections from drug targets to the hypertrophy network model. Drug candidates
75 with either no listed protein targets or no targets with directed protein interactions were excluded.
76 LogiRx identified top scoring directed pathways from drug targets to the hypertrophy signaling network
77 nodes through Omnipath using the PathLinker algorithm[27,28] in Cytoscape[29]. PathLinker computes a

78 ranked list of pathways by searching a directed protein interaction network, minimizing a cost function
79 of the product of edge weights along each candidate pathway[27,28]. Top scoring candidate drug pathways
80 were added to a LogiRx-expanded logic-based network model using Netflux.

81 **Literature validation of LogiRx-expanded models**

82 The LogiRx-expanded logic-based differential equation model was simulated to test the
83 functional impact of the drug pathways on cardiomyocyte hypertrophy. Each pathway was individually
84 added to the signaling network model to create expanded logic-based differential equation model
85 variants. Each drug-pathway-expanded model was simulated to predict the semi-quantitative network
86 dynamics in response to drug. To assess the functional validity of the LogiRx-identified drug pathways,
87 we validated their performance against 450 literature experiments previously used to validate the
88 hypertrophy signaling model[20].

89 **Simulating drug mechanisms of action**

90 Drug mechanisms of action were implemented using logic-based equations as described
91 previously[30,31], accounting for mechanisms of drug action (agonist or antagonist) and drug binding
92 (competitive or non-competitive). The binding properties determine how the upstream signal is shifted
93 by the drug dose, while the drug action determines whether the target node is upregulated (agonist) or
94 downregulated (antagonist). Each simulation was run first without drug input to establish baseline
95 activity, and then with the appropriate drug to identify steady-state changes in drug response.

96 **Mechanistic subnetwork analysis**

97 To identify pathways mediating drug response, we utilized the mechanistic subnetwork
98 method[30–32]. We simulated the global response of the network to the drug in the presence of
99 hypertrophic stimulus to identify “drug-responsive nodes”. We then simulated knockdown of each node
100 and measured that node’s influence on drug-induced change in cardiomyocyte hypertrophy, referring to
101 these nodes as “regulating nodes”. The intersection of the regulating nodes with responsive nodes

102 results in a mechanistic subnetwork that maps the pathways mediating drug activity. Thus, LogiRx
103 combines drug-target and protein interaction databases, path optimization, and logic-based network
104 simulations to obtain mechanistic subnetworks that explain drug response.

105 **Experimental validation in cardiomyocytes**

106 We isolated neonatal cardiomyocytes using the NeoMyts kit from Cellutron as described
107 previously[31]. Cardiomyocytes were cultured with serum for 24 hr in 96-well microplates, followed by a
108 24 hr serum starve. Cardiomyocytes were then treated with one of two hypertrophic stimuli (10 μM
109 phenylephrine, 5 ng/ml transforming growth factor β), 10% FBS (positive control), or serum-free media
110 alone (negative control). At the same time, cells were treated with specified concentrations of the
111 appropriate compound (escitalopram, mifepristone, paroxetine, sarpogrelate hydrochloride, or
112 AL082D06) for 48 hrs.

113 To prepare for immunofluorescent imaging, cardiomyocytes were first fixed with 4%
114 paraformaldehyde for 20 min, and then permeabilized with 0.1% Triton-X for 15 min. Cardiomyocytes
115 were blocked with 1% bovine serum albumin in PBS for 1 hr, then treated with mouse anti-α-actinin
116 primary antibody (Sigma-Aldrich Cat#A7811, RRID:AB_476766) at a concentration of 1:200 overnight.
117 Cardiomyocytes were blocked with 5% goat serum in PBS for 1 hr, then Alexa Fluor-568-conjugated goat
118 anti-mouse secondary antibody (Thermo Fisher Scientific Cat#A11031, RRID:AB_144696) at a
119 concentration of 1:200 was applied for 1 hr. The cells were stained with DAPI prior to imaging.

120 High-content imaging was performed on the stained cardiomyocytes using an Operetta CLS High
121 Content Analysis System. These images were processed using CellProfiler[33] using a cellular segmentation
122 algorithm developed previously and validated to within 5% of two independent manual
123 segmentations[34]. Median cell area was used as a representative measure of the cell population in each
124 well, and cells with undetectable cytoplasm were not counted.

125 **Patient outcomes associated with drug treatments**

126 To examine whether drugs were correlated with a reduction in cardiac adverse events
127 associated with hypertrophy, we analyzed data from two separate clinical databases. As the first patient
128 cohort, data was collected on November 30th, 2023 from the FDA's Adverse Event Reporting System
129 using the AERSMine tool[35]. The Adverse Event Reporting System is a multi-cohort database containing
130 20 million reports of adverse events from healthcare providers and consumers across the United States.
131 As a second patient cohort, on January 2nd, 2024 we collected data from the University of Virginia Health
132 System Network using the TriNetX tool, which provided access to electronic medical records from
133 approximately 1.7 million patients.
134 This retrospective study is exempt from informed consent. The data reviewed is a secondary
135 analysis of existing data, does not involve intervention or interaction with human subjects, and is de-
136 identified per the de-identification standard defined in Section §164.514(a) of the HIPAA Privacy Rule.
137 The process by which the data is de-identified is attested to through a formal determination by a
138 qualified expert as defined in Section §164.514(b)(1) of the HIPAA Privacy Rule. This formal
139 determination by a qualified expert refreshed on December 2020.
140 **Angiotensin II / Phenylephrine Infusion in Mice**
141 All animal procedures were performed in accordance with the Institutional Animal Care and Use
142 Committee at the University of Colorado Anschutz Medical Campus. Ten-week-old male C57BL/6J were
143 purchased from The Jackson Laboratory (Strain # 000664). Alzet mini-osmotic pumps (Model 2004), or
144 mock pumps for Sham animals, were implanted in a subcutaneous pocket created at the suprascapular
145 region under isoflurane anesthesia. Osmotic pumps were prepared to deliver 1.5 μg/kg/day Angiotensin
146 II (Bachem H-1705.0100) and 50 μg/g/day (R)-(-)-Phenylephrine hydrochloride (Sigma P6126) to induce
147 systemic hypertension, cardiac hypertrophy and fibrosis. Beginning 24 hours post-osmotic pump
148 implantation, animals were randomly divided into groups receiving 10 mg/kg/day escitalopram oxalate

149 (Selleckchem S4064) in 10% DMSO dissolved in 10% (2-hydroxypropyl) β-cyclodextrin (Sigma H107) in
150 water, or vehicle control, for 14 days.

151 **Echocardiographic Assessment of Cardiac Structure and Function**

152 Serial transthoracic echocardiographic and Doppler analysis were performed using the
153 VisualSonics Vevo F2 instrument. Animals were anesthetized with 2% isoflurane, hair on the chest was
154 removed using a chemical depilatory, and body temperature maintained at 37°C. Isoflurane was
155 maintained at 1.5% throughout the procedure to ensure a consistent plane of anesthesia across
156 subjects. Parasternal long axis (PSLAX) and parasternal short axis (SAX) views of the left ventricle were
157 obtained; SAX two-dimensional views of the LV at the level of the papillary muscle were used to acquire
158 M-mode images. Anterior and posterior LV wall thickness and internal diameters were measured in
159 systole and diastole using these M-mode images. Mitral inflow Doppler signals and myocardial tissue
160 movement of the mitral annulus were obtained to calculate the ratio of early and active filling waves of
161 blood flow through the mitral valve and ventricular tissue velocity to assess cardiac diastolic function.
162 Speckle-tracking strain analyses were acquired from PSLAX B-mode videos. All echocardiographic
163 measurements and analyses were averaged from at least four cardiac cycles and analyses were
164 performed in a blinded manner by a dedicated small animal echocardiography team.

165 **Tissue Procurement**

166 At study endpoint, animals were sacrificed by exsanguination and hearts excised and placed in
167 ice-cold saline. Right ventricular (RV) tissue was dissected from the LV by cutting along the septum and
168 the outer wall of the LV, and all parts weighed. 50 mg base and apical biopsies of the LV were flash-
169 frozen in liquid nitrogen for subsequent biochemical analysis. A cross-section of the LV at the level of the
170 papillary muscles was fixed in 4% PFA in PBS overnight at 4°C followed by preservation in a 30% sucrose
171 solution and embedding in OCT.

172 **Histological Analyses**

173 Frozen tissue sections were cut at a thickness of 10 μm. To evaluate total ventricular fibrotic
174 area, cardiac sections were stained with Picrosirius red dye (0.1% Direct Red 80 in saturated picric acid
175 solution) for 1 hour at room temperature. Whole-heart images were acquired using the image stitching
176 feature on a Keyence BZ-X710 All-in-One Fluorescence Microscope. Fibrotic area was determined by
177 quantifying the ratio of positively stained (red) pixels to the total pixel number of each section (reported
178 as percent collagen content) using ImageJ. In addition, individual cardiomyocyte hypertrophy was
179 assessed by staining cardiac sections with Alexa Fluor 647 wheat germ agglutinin (ThermoFisher
180 W32466) according to manufacturer instructions. Briefly, sections were incubated in a 5.0 μg/mL WGA
181 conjugate solution in HBSS for 10 minutes at room temperature, followed by mounting in ProLong™
182 Glass Antifade Mountant (ThermoFisher P36980). Images were acquired at 40x magnification with the
183 left ventricular free wall using the Keyence BZ-X710 microscope, and individual cardiomyocyte area was
184 quantified using ImageJ.

185 **Immunoblotting**

186 Total protein was isolated from neonatal rat ventricular myocytes (NRVM) using RIPA lysis buffer
187 (25 mM Tris pH 7.6, 150 mM NaCl, 1% NP-40, 1% sodium deoxycholate and 0.1% SDS) supplemented
188 with Halt™ protease and phosphatase inhibitor cocktail (ThermoFisher 78442). Proteins were separated
189 using SDS-PAGE and transferred onto nitrocellulose membrane (0.45 μm, Thermo Scientific 88018).
190 Total protein was first evaluated using LI-COR Revert™ 520 Total Protein Stain (926-10021), followed by
191 blotting with antibodies directed against phosphorylated protein kinase D (1:1,000; CST 2051) and
192 glyceraldehyde phosphate dehydrogenase (1:5,000; Proteintech 60004-1-Ig) overnight at 4°C in
193 intercept® (TBS) Blocking Buffer (LI-COR 927-60001) containing 0.2% Tween-20. Following incubation
194 with primary antibodies, blots were rinsed and probed with appropriate IRDye® secondary antibodies
195 (LI-COR). Protein bands were visualized using a LI-COR Odyssey XF scanner.

196 **Statistics**

197 All data are presented as the mean ± SEM. Analysis of experimental conditions considered two
198 distinct cardiomyocyte isolations and multiple conditions, with multiple wells in each experiment. For
199 this reason, a two-way ANOVA followed by Dunnett's test for multiple comparisons was selected for
200 statistical calculation. In vivo data were analyzed by ordinary one-way ANOVA followed by Tukey's
201 multiple comparisons test. GraphPad Prism 9 was used for statistical analysis. For all analyses, a p-value
202 <0.05 was considered statistically significant.
203
204 **RESULTS**
205 **Identified drug pathways driving cardiomyocyte hypertrophy**
206 Previously, we performed a microscopy-based screen for drugs that decreased hypertrophy of
207 cardiomyocytes in the presence of phenylephrine[12]. In that study, 94 of 3241 small molecule compounds
208 decreased both cell area and ANP protein expression by at least 70% and did not exhibit cardiotoxicity.
209 In a previous study, we identified that the hypertrophy signaling model was directly targeted by 32 of
210 these 94 drugs, and that the model could mechanistically predict reduction in hypertrophy with 88% (28
211 of 32) prediction accuracy [31]. The remaining 62 of 94 compounds do not target this previous
212 hypertrophy model and presumably inhibit cardiomyocyte hypertrophy through less-characterized
213 mechanisms. Therefore, in this study we sought to identify novel pathways linking the remaining 62
214 compounds to hypertrophy. To identify new drug pathways, we developed a logic-based network
215 predictor of drug pathways (LogiRx) that identifies and simulates molecular pathways that mediate how
216 drugs regulate cell phenotype.
217 As a first application, we employed LogiRx to identify proteins that are directly targeted by the
218 62 anti-hypertrophic compounds from our prior screen[12]. LogiRx analysis mapped 28 of the 62
219 compounds to 79 protein targets in the OmniPath protein interaction database (**Figure 1A**). 11 of 28
220 compounds were successfully mapped to the hypertrophy network via 214 candidate drug pathways

221 (**Figure 1B**). These pathways link 11 drugs and their drug targets to 89 proteins in the network, covering

222 42% of the network. Most of the candidate drug pathways (76%) connect the drug target to the

223 network via an intermediate protein that is not in the original network model, demonstrating the value

224 of pathway inference. Together, the 214 candidate drug-target-network pathways predict mechanisms

225 that may help explain the experimentally-demonstrated anti-hypertrophic effect of these 11

226 compounds.

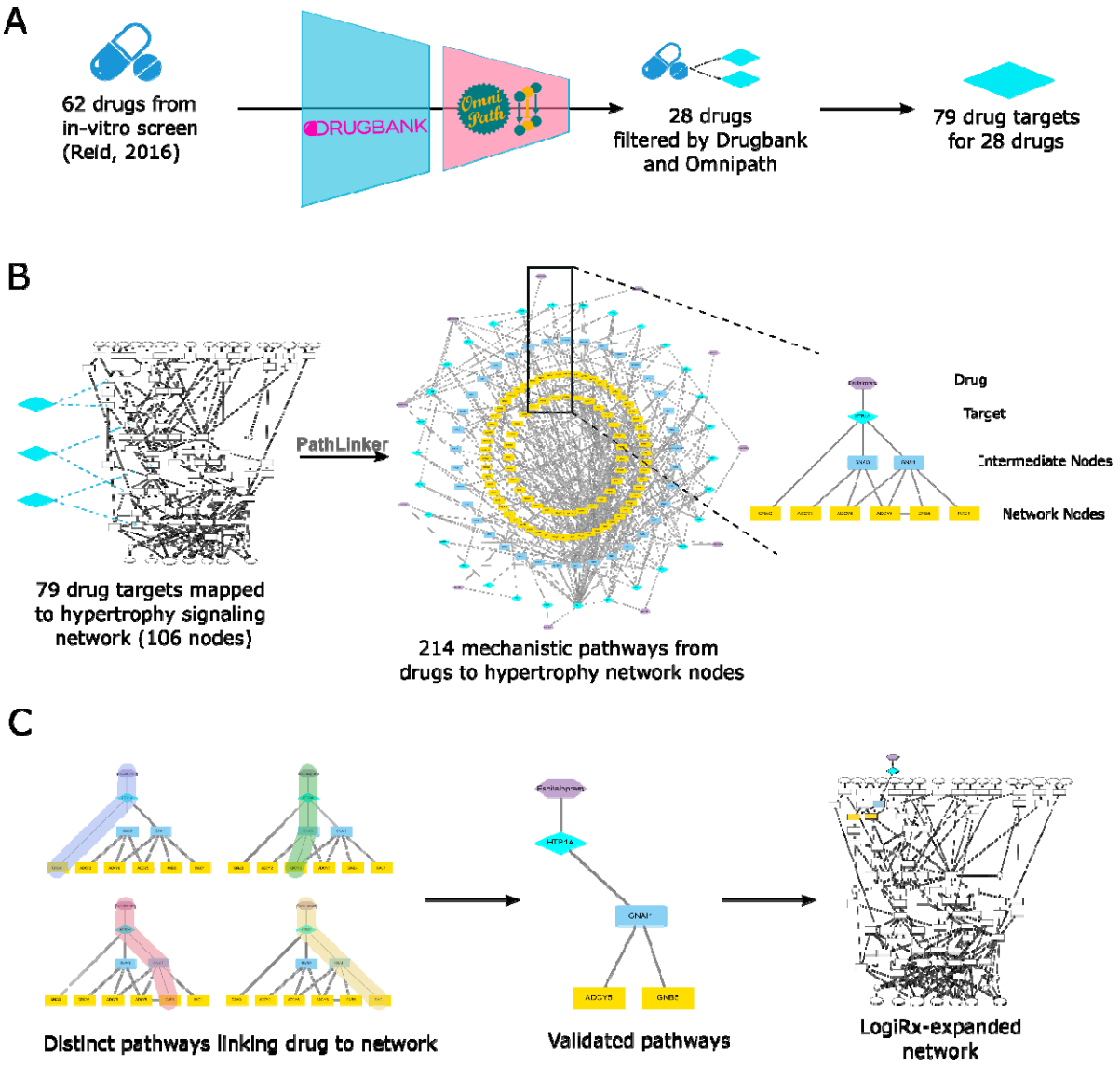

227

228 **Figure 1. LogiRx discovers pathways from anti-hypertrophic drugs to the cardiomyocyte hypertrophy**
229 **signaling network.** A) Drug targets are identified from DrugBank and filtered by annotations in the
230 protein-interaction database Omnipath. B) Drugs and their protein targets are mapped to the
231 hypertrophy network through LogiRx. C) Drug pathways are individually simulated using Netflux and
232 validated against prior experimental literature. Drug pathways that do not reduce model validation are
233 used to expand the hypertrophy network for drug predictions.
234
235 **Logic-based network expansion to predict how drugs regulate hypertrophy**
236 To predict the impact of these drug pathways on cardiomyocyte hypertrophy, logic-based
237 differential equation model variants were created from LogiRx that each simulate the effect of
238 incorporating individual pathway (**Figure 1C**). Each model variant was tested by simulating inhibition of
239 the drug target in the presence of hypertrophic agonist phenylephrine. Most drug pathways were
240 predicted to strongly inhibit hypertrophy (**Figure 2A**). However, some drug pathways reduced the model
241 accuracy when tested against a previous set of 450 experiments, indicating that they are not fully
242 compatible with the mechanisms established in the validated network model (**Figure 2A**).
243 Drug pathways corresponding to 8 of the 11 drugs were predicted to inhibit phenylephrine-
244 induced hypertrophy while maintaining model accuracy above 78%. New LogiRx-expanded drug models
245 were developed combining all relevant validated pathways for each of the 8 drugs. The hypertrophic
246 effect of each drug was simulated using a pharmacological inhibition model based on known drug-target
247 binding mechanisms[30]. Seven of these eight drugs were predicted to be anti-hypertrophic, with context-
248 dependent efficacy depending on the hypertrophic stimulus (**Figure 2B**). 7 of 8 drugs regulated
249 hypertrophy via multiple protein targets.
250

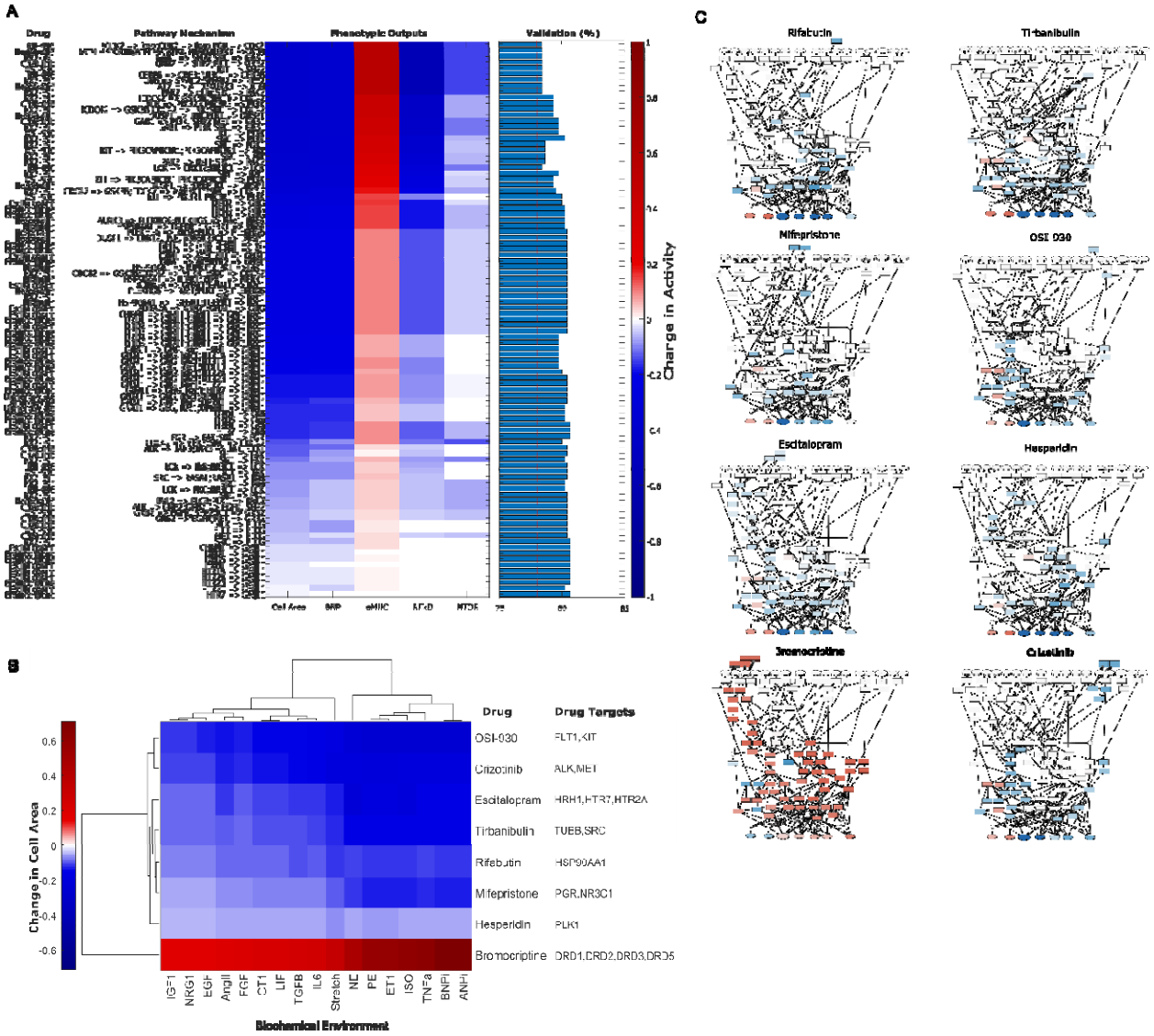

Figure 2. LogiRx-based network model expansion predicts pathways by which drugs affect cardiomyocyte hypertrophy. A) Hypertrophy network variants expanded by individual pathways were simulated for their effect on five hypertrophic outputs, as well as validated against 450 experiments from prior literature. B) 8 drugs were predicted to affect cardiomyocyte hypertrophy with varying efficacy across 17 biochemical environments. C) Drugs were predicted to inhibit hypertrophy via distinct regional modulation of the hypertrophy signaling network, indicating distinct inhibitory mechanisms.

259 Seven drugs were predicted by the LogiRx-expanded network model to inhibit hypertrophy –
260 OSI-930, crizotinib, escitalopram, tirbanibulin, rifabutin, mifepristone, and hesperidin, representing a
261 variety of drug targets and clinical applications. OSI-930 is an FLT1 and KIT inhibitor that is designed to
262 target cancer cell proliferation in solid tumors[36]. Crizotinib, an ALK and MET inhibitor, is used to treat
263 non-small cell lung cancer but has known cardiac toxicity[37,38]. Escitalopram targets SERT and is used to
264 treat depression and anxiety[39,40]. Tirbanibulin targets TUBB and SRC to treat actinic keratosis, and is
265 being investigated as a potential treatment for acute myeloid leukemia[41]. Rifabutin inhibits HSP90AA1
266 and is an antibiotic preventing mycobacterium avium complex in HIV patients[42]. Mifepristone, which
267 targets both PGR and NR3C1, is commonly used as an abortifacient, but is additionally used to treat
268 diabetic patients with Cushing's syndrome[43]. Hesperidin is a flavonoid and natural supplement currently
269 investigated for anti-inflammatory benefits[44]. Similar to their target diversity, these 8 drugs were
270 predicted to inhibit cardiomyocyte hypertrophy through distinct areas of the hypertrophy network
271 (**Figure 2C**).
272
273 **Experiments in cardiomyocytes validate that escitalopram and mifepristone inhibit hypertrophy**
274 We further prioritized escitalopram, tirbanibulin, mifepristone, OSI-930, and rifabutin for
275 experimental validation based on their relative cardiac safety[36,45–50] and approval status. Neonatal rat
276 cardiomyocytes were treated with PE along with each of these five drugs for 48 h. Consistent with the
277 LogiRx model predictions, tirbanibulin, escitalopram, and mifepristone inhibited PE-induced
278 cardiomyocyte hypertrophy (**Figure 3A-B**). In contrast, OSI-930 and rifabutin did not inhibit hypertrophy
279 even at increased concentrations.
280 While the network analysis in **Figure 2C** predicted that escitalopram would work via
281 downstream hypertrophic pathways that are relatively context-independent, an alternative hypothesis
282 may suggest that escitalopram inhibits alpha-1 adrenergic receptor (α1AR) directly in response to

283 phenylephrine. We tested this hypothesis by introducing an alternative hypertrophic stimulus TGFβ, as
284 well as directly measuring phosphorylation of protein kinase D (PKD), which is proximal to the α1
285 adrenergic receptor in cardiomyocytes. TGFβ-induced hypertrophy was inhibited by both escitalopram
286 and mifepristone (**Figure 3C-D**). Further, while we observed a robust increase in phospho-PKD levels in
287 cardiomyocytes treated with phenylephrine stimulation, no reduction in PKD phosphorylation was
288 observed in cardiomyocytes co-treated with escitalopram. Together, these data indicate that
289 escitalopram antagonizes hypertrophy through downstream mechanisms distinct from blockade of the
290 α1AR.

291 To identify how mifepristone inhibits cardiomyocyte hypertrophy, we performed mechanistic
292 subnetwork analysis. Although the LogiRx network model included drug pathways for mifepristone via
293 both progesterone receptors and glucocorticoid receptors, LogiRx predicted that mifepristone inhibits
294 cardiomyocyte hypertrophy predominantly via inhibition of the glucocorticoid receptor via LCK/ERK and
295 CEBPβ (**Supplemental Figure 1A-B**). We experimentally validated that the glucocorticoid receptor
296 antagonist AL082D06 phenocopied the effects of mifepristone by preventing hypertrophy with PHE or
297 TGFβ (**Supplemental Figure 1C-D**).

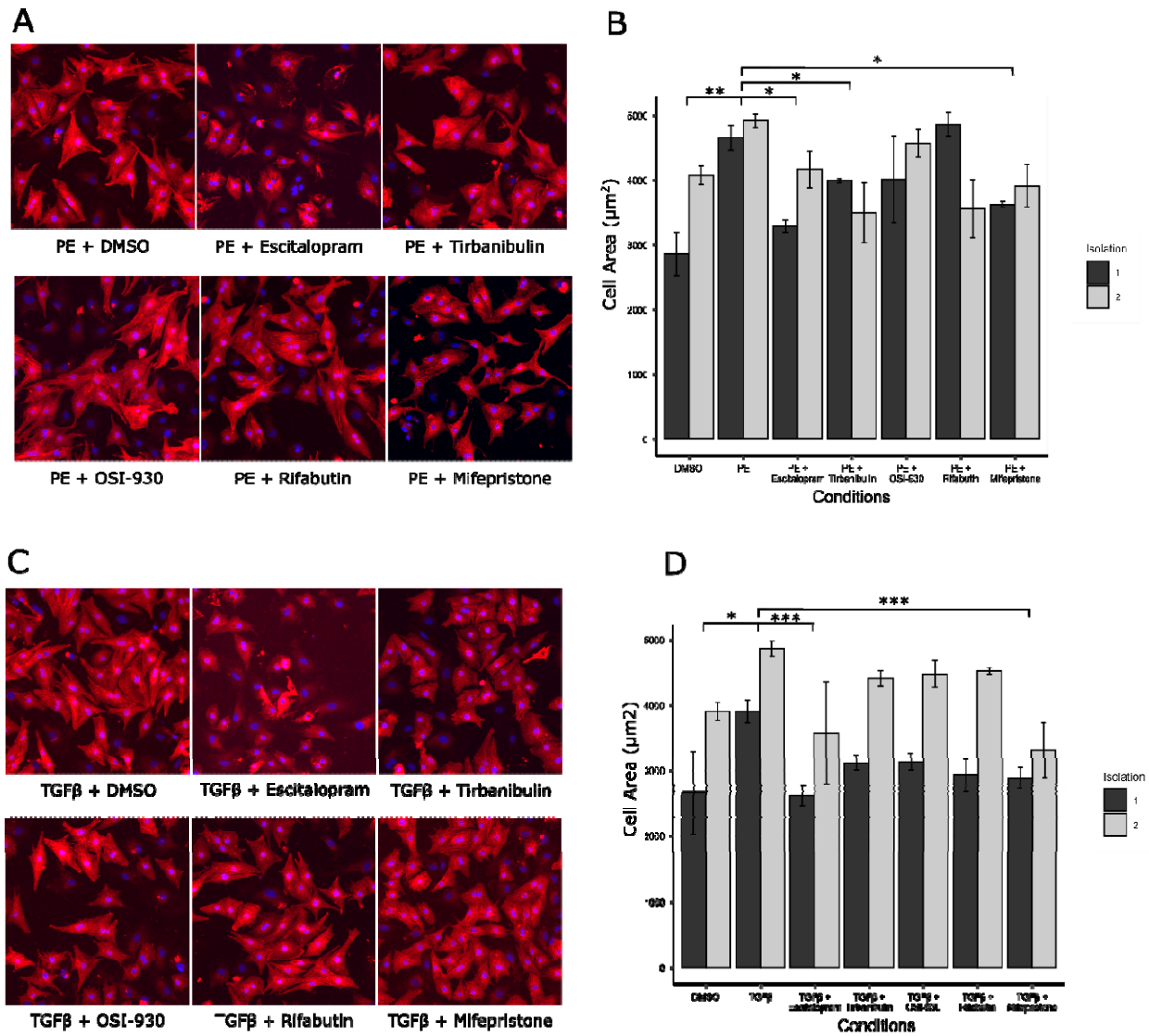

Figure 3. Escitalopram and mifepristone inhibit cardiomyocyte hypertrophy induced by either phenylephrine or TGFβ. The effect of five drugs on PE-induced hypertrophy of neonatal rat cardiomyocytes is shown in A) representative images or B) quantification of automated segmentation. Escitalopram (20 µM), mifepristone (6 µM), and tirbanibulin (6 µM) significantly prevented PE-induced cell area increase over a 48-hour period following treatment. The effect of these five drugs on TGFβ-induced hypertrophy is shown as C) representative images or D) quantification of cardiomyocyte cell area by automated segmentation. Escitalopram (20 µM) and mifepristone (6 µM) significantly prevented TGFβ-induced increase in cell area. Two cell isolations were used for each experiment, and a two-way

307 ANOVA was performed followed by a Dunnett's post-hoc test. Error bar indicates SEM, * $p<0.05$, **
308 $p<0.01$, *** $p<0.001$.
309
310 **Escitalopram inhibits hypertrophy through serotonin receptor and not transporter**
311 As the last stage of LogiRx, we performed mechanistic subnetwork analysis to identify pathways
312 that mediate escitalopram inhibition of cardiomyocyte hypertrophy. We simulated the network-wide
313 response to escitalopram, followed by simulations of network-wide knockdown of each network node in
314 the presence and absence of escitalopram. The intersection of these two analyses resulted in a
315 mechanistic subnetwork that predicted how escitalopram inhibits cardiomyocyte hypertrophy (**Figure**
316 **4A**). This subnetwork predicted that escitalopram inhibits hypertrophy through the serotonin receptor
317 HT2RA, a non-canonical target of escitalopram, rather than as a selective serotonin reuptake inhibitor
318 (SSRI) via the transporter SERT (or SLC6A4). Further, the LogiRx model predicted that the escitalopram-
319 HTR2A pathway acts by inhibiting G-protein signaling to PI3Kγ (**Figure 4A-B**).
320 To experimentally validate these LogiRx predictions, we used sarpogrelate hydrochloride which
321 selectively inhibits HTR2A but not SERT. Prior literature[51,52] demonstrates that sarpogrelate inhibits PE-
322 induced cardiomyocyte hypertrophy both in vitro and in vivo. Our studies confirm that sarpogrelate
323 prevents both PE- and further demonstrates its efficacy against TGFβ-induced cardiomyocyte
324 hypertrophy (**Figure 4C-D**). Downstream of HTR2A, our mechanistic subnetwork predicted Gβγ and PI3K
325 to mediate anti-hypertrophic escitalopram activity. Gβγ directly binds and activates PI3Kγ[53]. To
326 experimentally validate this prediction, we selectively inhibited PI3Kγ with the antitumor drug
327 eganelisib. Eganelisib prevented both PE- and TGFβ-induced cardiomyocyte hypertrophy (**Figure 4E-F**),
328 further validating the non-canonical escitalopram-HTR2A-PI3Kγ pathway predicted by LogiRx.

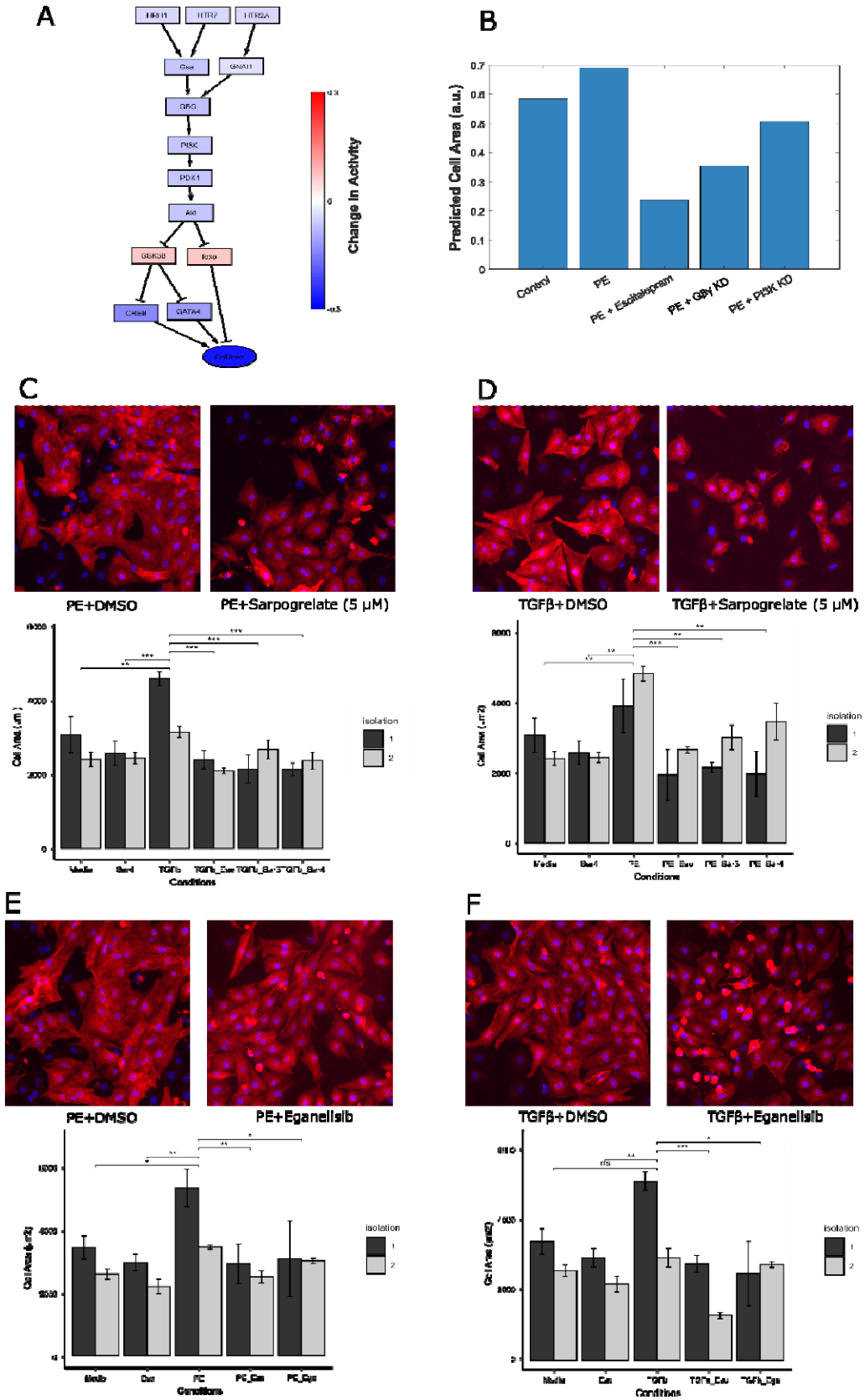
A
B
Predicted Cell Area (a.u.)
Control
PE
PE + Escitalopram
PE + GBy KD
PE + PI3K KD
Change in Activity
C
D
PE+DMSO
PE+Sarpogrelate (5 μM)
TGFβ+DMSO
TGFβ+Sarpogrelate (5 μM)
isolation
Conditions
E
F
PE+DMSO
PE+Eganelisib
TGFβ+DMSO
TGFβ+Eganelisib

330 **Figure 4. Escitalopram prevents cardiomyocyte hypertrophy by inhibiting serotonin receptors.** A)
331 Mechanistic subnetwork analysis to predict how escitalopram suppresses cardiomyocyte hypertrophy.
332 B) Simulations of PE-induced hypertrophy and modulation by escitalopram, Gβγ inhibition, or PI3Kγ
333 inhibition. Serotonin receptor inhibitor sarpogrelate hydrochloride (5 µM) significantly prevents C) PE-
334 and D) TGFβ-induced cardiomyocyte hypertrophy 48 hours post treatment, as shown by representative
335 images and quantification of automated segmentation. PI3Kγ inhibitor eganelisib (20 µM) significantly
336 prevents E) PE- and F) TGFβ-induced cardiomyocyte hypertrophy 48 hours post treatment, as shown by
337 representative images and quantification of automated segmentation. Two cell isolations were used for
338 each experiment, and a two-way ANOVA was performed followed by a Dunnett's post-hoc test. Error
339 bar indicates SEM, * $p<0.05$, ** $p<0.01$, *** $p<0.001$.
340
341 **Escitalopram inhibits cardiomyocyte hypertrophy *in vivo***
342 To test whether escitalopram also reduces cardiomyocyte hypertrophy in vivo, escitalopram was
343 delivered to mice subjected to the angiotensin II and phenylephrine (AngII/PE) as a mouse model of
344 cardiac hypertrophy and fibrosis. Angiotensin II (1.5 mg/kg/day) and phenylephrine (50 mg/kg/day)
345 were delivered continuously for 14 days through an osmotic minipump as previously described[54]; daily
346 escitalopram was administered via intraperitoneal injection at 10 mg/kg/day beginning the day after
347 pump implantation (**Figure 5A**). Mice subjected to AngII/PE for 14 days exhibited significant global
348 cardiac hypertrophy, as indicated by heart weight to body weight ratio (HW:BW), as well as a significant
349 increase in LV mass in particular (LV:TL) (**Figure 5B-C**). Furthermore, AngII/PE challenge induced
350 dramatic fibrosis in the LV free wall, which likely also contributed to the increase in overall LV mass
351 (**Figure 5D-E**). Cardiac structure and systolic and diastolic function were evaluated by echocardiography,
352 revealing an increase in LV wall thickness in diastole, which is consistent with the increased HW:BW
353 ratio (**Figure 5F**). Furthermore, AngII/PE mice demonstrated trends towards increases in systolic

354 function, measured by ejection fraction, as well as increases in the E/E' ratio, which is indicative of
355 impaired LV relaxation or diastolic dysfunction (**Figure 5G-H**).
356 Some mice treated with AngII/PE also received daily administration of escitalopram delivered via
357 intraperitoneal injection at 10 mg/kg/day. These animals showed no change in overall collagen content
358 in the LV, suggesting a lack of an effect on the cardiac fibroblast population (**Figure 5D-E**). There was
359 also no significant effect of escitalopram on global cardiac hypertrophy or any functional parameters
360 assessed by echocardiography (**Figure 5B-C,F-H**). However, imaging of cardiomyocyte sections stained
361 with WGA revealed a modest but significant reduction in individual cardiomyocyte hypertrophy in
362 response to treatment with escitalopram (**Figure 5I-J**). In summary, while escitalopram did not offer
363 significant protection against global cardiac hypertrophy or dysfunction in this severe injury model,
364 escitalopram attenuated cardiomyocyte hypertrophy in vivo, consistent with the antihypertrophic effect
365 of escitalopram predicted by LogiRx and measured in cultured cardiomyocytes.
366

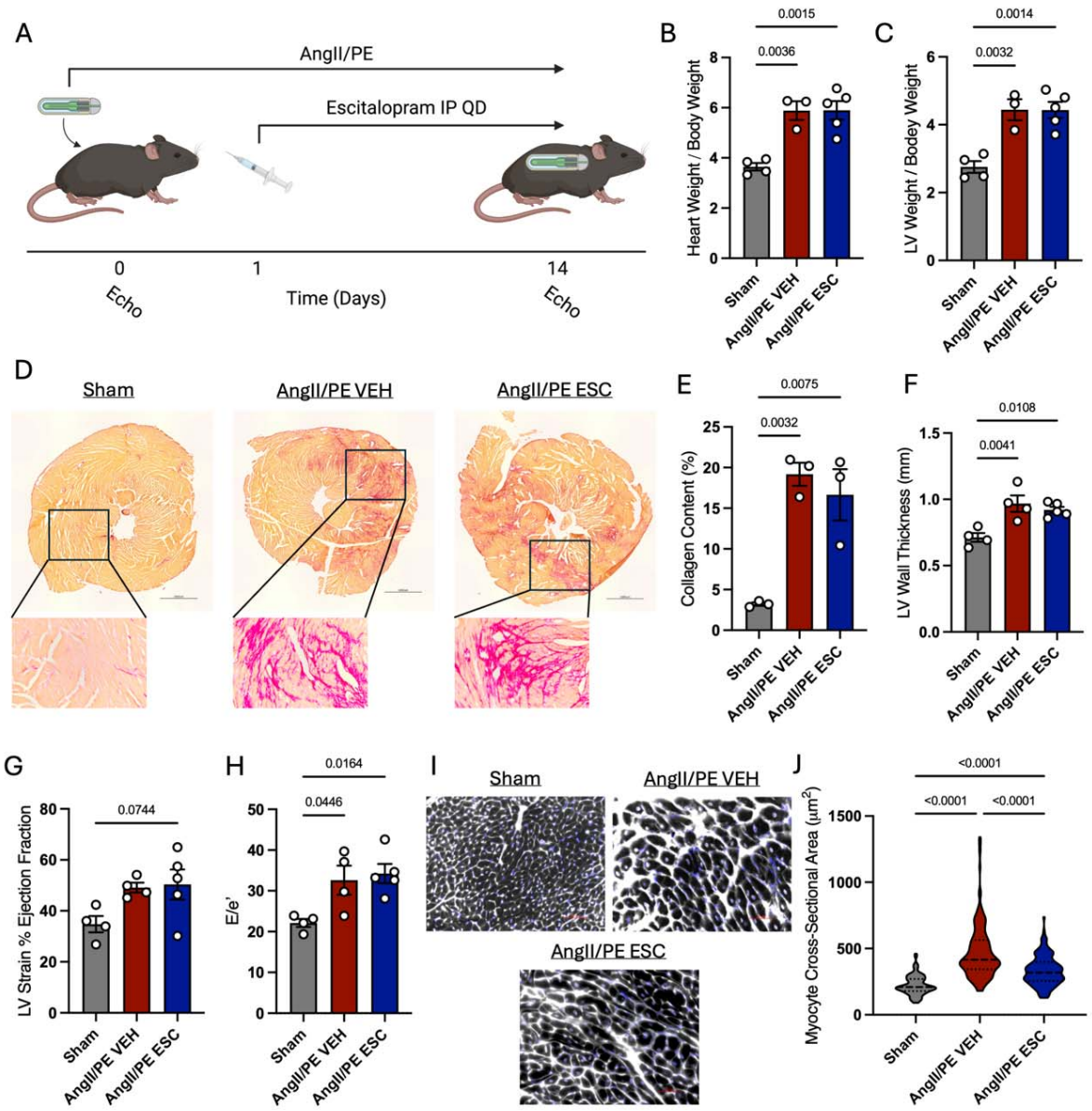

Figure 5. Escitalopram Attenuates Cardiomyocyte Hypertrophy in AngII/PE Mice

A. Schematic of cardiac injury model and escitalopram administration. Mice were continuously delivered AngII/PE through an osmotic minipump to induce cardiac injury and fibrosis, and injected with 10 mg/kg/day escitalopram or vehicle control for 14 days. Quantification of HW:BW (B) and LV:BW (C) ratios. D. Representative picrosirius red staining of heart cross-sectional tissues in sham mice and AngII/PE mice treated with vehicle or escitalopram, and quantification of percent collagen content (E). Results of echocardiographic analyses of AngII/PE mice, showing the left ventricular wall thickness in

374 diastole (F), percent ejection fraction derived from strain analysis (G), and the ratio of early mitral valve
375 flow velocity to mitral annulus velocity by tissue Doppler (E/e') indicating diastolic function. I. Wheat
376 germ agglutinin staining of tissue sections, with quantification of cardiomyocyte cross-sectional area (J).
377 Statistical analyses performed by one-way ANOVA with Tukey's post hoc multiple comparisons test.
378
379 **Cardiac outcomes for patients prescribed escitalopram**
380 Based on consistent anti-hypertrophic roles of escitalopram shown by LogiRx, cultured rat
381 cardiomyocytes, and mouse cardiomyocytes in vivo, we asked whether patients prescribed escitalopram
382 may also exhibit a reduced incidence of cardiac hypertrophy. We first mined patient reports from the
383 FDA Adverse Event Reporting System for incidence of cardiac hypertrophy or failure among patients
384 prescribed escitalopram or related SSRIs that are not known to target HTR2A. Among those diagnosed
385 with depression, patients prescribed escitalopram (which inhibits both SERT and HTR2A) had a lower
386 incidence of left ventricular or ventricular hypertrophy when compared to treatment with other SSRIs
387 sertraline, venlafaxine, and paroxetine that inhibit SERT but not HTR2A (**Figure 6A**). An exception is
388 patients treated with fluoxetine, who had lower incidence of cardiac failure compared to escitalopram
389 treatment.
390 To validate these findings in an independent patient population with more structured data
391 collection, we mined electronic health records from the University of Virginia (UVA) Health System.
392 Among UVA patients diagnosed with depression, those prescribed escitalopram exhibited a statistically
393 lower incidence of left ventricular hypertrophy than those prescribed SSRI paroxetine as well as the
394 serotonin receptor agonist buspirone (**Figure 6B**). To verify the hypertrophy annotation from this
395 analysis, we examined echocardiograms from de-identified patients using the same drug and diagnosis
396 queries. These confirm qualitatively larger interventricular septum thickness (IVSD) and left ventricular
397 posterior wall end diastole (LVPWD) in a patient prescribed paroxetene and diagnosed with hypertrophy

than echocardiograms from patients prescribed escitalopram or other SSRIs not diagnosed with hypertrophy (**Figure 6C**).Stratifying patients in the FDA (**Figure 6D**) and UVA (**Figure 6E**) databases by sex, both male and female patients prescribed escitalopram exhibit less hypertrophy than that seen with two or more SSRIs.

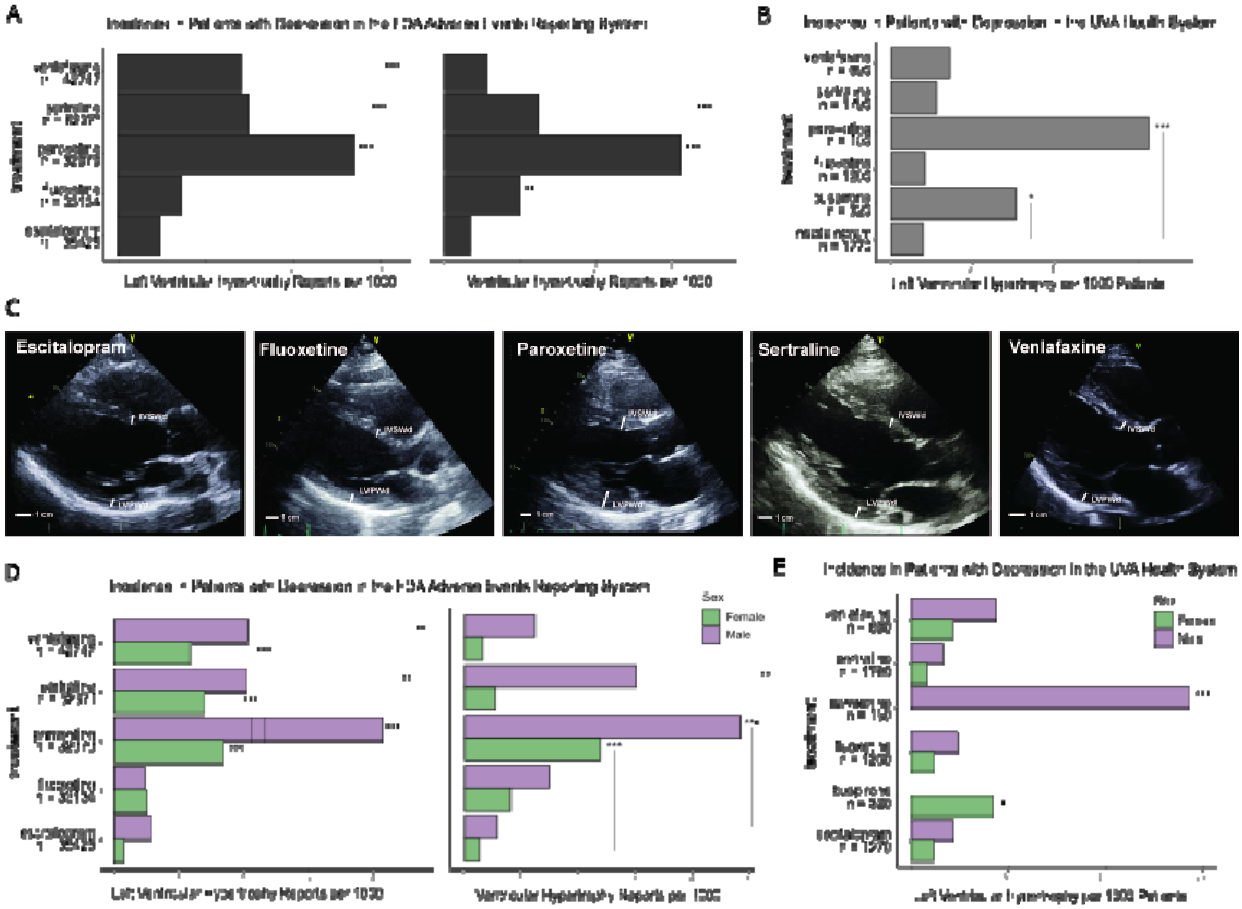

Figure 6. In two patient cohorts with depression, those prescribed escitalopram exhibit a lower incidence of cardiac hypertrophy than those prescribed other SSRIs. A) Reports of left ventricular hypertrophy (left) or ventricular hypertrophy (right) per 1000 patients are shown for patients with depression taking either escitalopram or another SSRI (fluoxetine, paroxetine, sertraline, or venlafaxine) in the FDA Adverse Events Reporting System. B) Diagnoses of left ventricular hypertrophy per 1000 patients are shown for patients with depression taking either escitalopram or another SSRI in the U. Virginia Health System. C) Verification of echocardiograms from patients in the UVA Health System with

410 hypertrophy (prescribed paroxetine) or without hypertrophy (prescribed escitalopram, fluoxetine,
411 sertraline, or venlafaxine). D) FDA adverse event reports of left ventricular hypertrophy (left) or
412 ventricular hypertrophy (right) per 1000 patients are further divided into incidence by sex. E) Diagnoses
413 of left ventricular hypertrophy in the UVA Health System, divided into incidence by sex. In the UVA
414 Health System, no female patients prescribed paroxetine and no male patients prescribed busipirone
415 exhibited left ventricular hypertrophy. * $p<0.05$, ** $p<0.01$, *** $p<0.001$.
416

417 **Discussion**

418 Despite a strong association between heart failure and hypertrophy, drugs that directly treat
419 hypertrophy are limited[55]. As seen with sildenafil, drug repurposing may provide a rapid translational
420 avenue to identify new therapeutic strategies for cardiac hypertrophy and heart failure[56,57]. Drug
421 repurposing requires sophisticated screening for efficacy but also methods to identify how effective
422 drugs work. In this study we developed a new mechanistic machine learning method, LogiRx, that
423 predicts new pathways that map from drugs to a mechanistic logic-based model of a signaling network.
424 We applied LogiRx to hits from our previous experimental compound screen[12] and predicted the
425 pathways by which 7 of these drugs modulate cardiomyocyte hypertrophy. Experiments in cultured
426 cardiomyocytes validated the context-independent antihypertrophic role of two drugs, escitalopram and
427 mifepristone predicted by LogiRx. Pathways that mediate the effects of escitalopram and mifepristone
428 were predicted by subnetwork analysis, and these predictions were further experimentally validated
429 (escitalopram: serotonin receptors and Gβγ; mifepristone: glucocorticoid receptor). Analysis of
430 electronic health records validate these in silico and in vitro results findings, demonstrating that
431 escitalopram is associated with a lower incidence of cardiac hypertrophy in depression or anxiety
432 patients compared to multiple SSRIs in two large independent populations. Together, these results
433 suggest potential repurposing avenues for escitalopram and mifepristone in cardiac hypertrophy.

434 LogiRx identifies regulatory signaling pathways and dynamic mechanistic predictions that map
435 from drugs to an established signaling network. Several other computational methods construct
436 signaling pathways from both protein-interaction and/or gene expression data[58–60]. Notably, CARNIVAL
437 combines gene expression with protein interaction data to predict upstream signaling pathways that
438 drive changes gene expression changes[61]. LogiRx provides additional benefits of its logic-based
439 differential equation framework that is highly validated for cardiomyocyte hypertrophy[19,20,31,62] to
440 provide dynamic, mechanistic simulations of perturbation experiments (**Figure 2, 4**).
441 Escitalopram (Lexapro) is a commonly prescribed SSRI (>30M prescriptions in the US) with a
442 well-known safety profile[39,40]. Less well understood is the role of SSRIs in cardiac disease. Escitalopram
443 was shown to prevent a diabetic model of cardiac hypertrophy, however the mechanisms remain poorly
444 understood[63]. Our LogiRx model predicts that escitalopram inhibits cardiomyocyte hypertrophy through
445 its off-target HTR2A. This predicted mechanism is supported by our understanding of the role of
446 serotonin receptors HTR2A and HTR2B[64–66] in cardiomyocyte hypertrophy. Paroxetine, another SSRI that
447 more specifically targets SERT, was previously shown to prevent left ventricular dysfunction following
448 myocardial infarction through an off-target GRK2 mechanism[67]. GRK2 is unlikely to mediate the
449 increased incidence of hypertrophy we found associated with patients prescribed paroxetine, because
450 the clinical concentration is below the IC50 for GRK2[68,69]. Escitalopram off-target of HT2A and paroxetine
451 off-target of GRK2 indicates that other SSRIs may have off-targets that contribute to the differential
452 association with cardiac hypertrophy and failure we observed in patients with depression or anxiety.
453 Further, paroxetine derivatives with enhanced affinity for GRK2 demonstrate the potential for selective
454 repurposing towards "off targets"[70,71].
455 While mifepristone is best known as a progesterone inhibitor, it was originally discovered in a
456 search for glucocorticoid receptor antagonists and is used in Cushing's syndrome with hyperglycemia[43].
457 Glucocorticoids and their receptors have a complex role in cardiovascular health. Glucocorticoid

458 stimulation induces hypertrophy in primary rat cardiomyocytes[72,73], yet mice with cardiomyocyte-
459 specific deletion of glucocorticoid receptor have increased cardiac hypertrophy[74] and direct
460 glucocorticoid receptor inhibition can enhance cardiomyocyte proliferation[75]. LogiRx predicted that
461 mifepristone inhibits cardiomyocyte hypertrophy through a glucocorticoid receptor - LCK – ERK
462 pathway, which we validated in two contexts in cultured cardiomyocytes. The implications of
463 mifepristone for repurposing against cardiac hypertrophy warrant further investigation.
464 Machine learning methods that not only predict efficacy but also pathway mechanisms are
465 greatly needed. Here, we developed a mechanistic machine learning method LogiRx to discover
466 pathways by which escitalopram and mifepristone inhibit cardiomyocyte hypertrophy. These pathways
467 were validated in cultured cells in two contexts. Escitalopram decreased cardiomyocyte hypertrophy in
468 vivo and was associated with a lower incidence of cardiac hypertrophy in two patient cohorts. Together,
469 these studies demonstrate the ability of LogiRx to predict drug efficacy and mechanisms that guide new
470 experiments.
471

472 **Acknowledgments**

473 We thank Mohammad Fallahi-Sichani for use of his Perkin Elmer Operetta, statistical consulting from
474 Marieke Jones, and Malcom O'Malley for naming LogiRx.
475

476 **References**

477 1. Frey, N., Katus, H. A., Olson, E. N. & Hill, J. A. Hypertrophy of the Heart. *Circulation* **109**, 1580–1589
478 (2004).
479 2. Samak, M. *et al.* Cardiac Hypertrophy: An Introduction to Molecular and Cellular Basis. *Med. Sci.*
480 *Monit. Basic Res.* **22**, 75–79 (2016).

481 3. Nomura, S. *et al.* Cardiomyocyte gene programs encoding morphological and functional signatures in
482 cardiac hypertrophy and failure. *Nat. Commun.* **9**, 4435 (2018).
483 4. Marian, A. J. 23 - Heart Failure as a Consequence of Hypertrophic Cardiomyopathy. in *Heart Failure: a*
484 *Companion to Braunwald's Heart Disease (Fourth Edition)* (eds. Felker, G. M. & Mann, D. L.) 311-
485 321.e6 (Elsevier, Philadelphia, 2020). doi:10.1016/B978-0-323-60987-6.00023-5.
486 5. Bazgir, F. *et al.* The Microenvironment of the Pathogenesis of Cardiac Hypertrophy. *Cells* **12**, 1780
487 (2023).
488 6. Xie, M., Burchfield, J. S. & Hill, J. A. Pathological Ventricular Remodeling: Mechanisms: Part 1 of 2.
489 *Circulation* **128**, 388–400 (2013).
490 7. Tham, Y. K., Bernardo, B. C., Ooi, J. Y. Y., Weeks, K. L. & McMullen, J. R. Pathophysiology of cardiac
491 hypertrophy and heart failure: signaling pathways and novel therapeutic targets. *Arch. Toxicol.* **89**,
492 1401–1438 (2015).
493 8. Tsao, C. W. *et al.* Heart Disease and Stroke Statistics-2023 Update: A Report From the American Heart
494 Association. *Circulation* **147**, e93–e621 (2023).
495 9. Schubert, M., Hansen, S., Leefmann, J. & Guan, K. Repurposing Antidiabetic Drugs for Cardiovascular
496 Disease. *Front. Physiol.* **11**, 568632 (2020).
497 10. Onódi, Z., Koch, S., Rubinstein, J., Ferdinandy, P. & Varga, Z. V. Drug repurposing for
498 cardiovascular diseases: New targets and indications for probenecid. *Br. J. Pharmacol.* **180**, 685–700
499 (2023).
500 11. Xie, Y. *et al.* Mechanisms of SGLT2 Inhibitors in Heart Failure and Their Clinical Value. *J.*
501 *Cardiovasc. Pharmacol.* **81**, 4–14 (2023).
502 12. Reid, B. G. *et al.* Discovery of novel small molecule inhibitors of cardiac hypertrophy using high
503 throughput, high content imaging. *J. Mol. Cell. Cardiol.* **97**, 106–113 (2016).

504 13. Dukinfield, M. *et al*. Repurposing an anti-cancer agent for the treatment of hypertrophic heart
505 disease. *J. Pathol.* **249**, 523–535 (2019).
506 14. Escudero, D. S. *et al.* PDE5 inhibition improves cardiac morphology and function in SHR by
507 reducing NHE1 activity: Repurposing Sildenafil for the treatment of hypertensive cardiac hypertrophy.
508 *Eur. J. Pharmacol.* **891**, 173724 (2021).
509 15. Wang, Z. *et al.* A high-throughput drug screening identifies luteolin as a therapeutic candidate
510 for pathological cardiac hypertrophy and heart failure. *Front. Cardiovasc. Med.* **10**, 1130635 (2023).
511 16. Nakamura, M. & Sadoshima, J. Mechanisms of physiological and pathological cardiac
512 hypertrophy. *Nat. Rev. Cardiol.* **15**, 387–407 (2018).
513 17. Sun, J., Yang, J., Chi, J., Ding, X. & Lv, N. Identification of drug repurposing candidates based on a
514 miRNA-mediated drug and pathway network for cardiac hypertrophy and acute myocardial
515 infarction. *Hum. Genomics* **12**, 52 (2018).
516 18. Rai, A., Kumar, V., Jerath, G., Kartha, C. C. & Ramakrishnan, V. Mapping drug-target interactions
517 and synergy in multi-molecular therapeutics for pressure-overload cardiac hypertrophy. *NPJ Syst.*
518 *Biol. Appl.* **7**, 11 (2021).
519 19. Ryall, K. *et al.* Network reconstruction and systems analysis of cardiac myocyte hypertrophy
520 signaling. *J. Biol. Chem.* **287**, 42259–42268 (2012).
521 20. Khalilimeybodi, A., Paap, A. M., Christiansen, S. L. M. & Saucerman, J. J. Context-specific network
522 modeling identifies new crosstalk in β-adrenergic cardiac hypertrophy. *PLoS Comput. Biol.* **16**, (2020).
523 21. Wishart, D. S. *et al.* DrugBank 5.0: a major update to the DrugBank database for 2018. *Nucleic*
524 *Acids Res.* **46**, D1074–D1082 (2018).
525 22. Türei, D., Korcsmáros, T. & Saez-Rodriguez, J. OmniPath: guidelines and gateway for literature-
526 curated signaling pathway resources. *Nat. Methods* **13**, 966–967 (2016).

527 23. Ceccarelli, F., Turei, D., Gabor, A. & Saez-Rodriguez, J. Bringing data from curated pathway
528 resources to Cytoscape with OmniPath. *Bioinformatics* **36**, 2632–2633 (2020).
529 24. Kanehisa, M. & Goto, S. KEGG: Kyoto Encyclopedia of Genes and Genomes. *Nucleic Acids Res.*
530 **28**, 27–30 (2000).
531 25. Haw, R., Hermjakob, H., D'Eustachio, P. & Stein, L. Reactome pathway analysis to enrich
532 biological discovery in proteomics data sets. *PROTEOMICS* **11**, 3598–3613 (2011).
533 26. Perfetto, L. *et al.* SIGNOR: a database of causal relationships between biological entities. *Nucleic*
534 *Acids Res.* **44**, D548–D554 (2016).
535 27. Gil, D. P., Law, J. N. & Murali, T. M. The PathLinker app: Connect the dots in protein interaction
536 networks. *F1000Research* **6**, 58 (2017).
537 28. Ritz, A. *et al.* Pathways on demand: automated reconstruction of human signaling networks. *NPJ*
538 *Syst. Biol. Appl.* **2**, 16002 (2016).
539 29. Shannon, P. *et al.* Cytoscape: A Software Environment for Integrated Models of Biomolecular
540 Interaction Networks. *Genome Res.* **13**, 2498–2504 (2003).
541 30. Zeigler, A. C. *et al.* Network model-based screen for FDA-approved drugs affecting cardiac
542 fibrosis. *CPT Pharmacomet. Syst. Pharmacol.* **10**, 377–388 (2021).
543 31. Eggertsen, T. G. & Saucerman, J. J. Virtual drug screen reveals context-dependent inhibition of
544 cardiomyocyte hypertrophy. *Br. J. Pharmacol.* **180**, 2721–2735 (2023).
545 32. Van de Graaf, M. W., Eggertsen, T. G., Zeigler, A. C., Tan, P. M. & Saucerman, J. J. Benchmarking
546 of protein interaction databases for integration with manually reconstructed signalling network
547 models. *J. Physiol.* (2023) doi:10.1113/JP284616.
548 33. Stirling, D. R. *et al.* CellProfiler 4: improvements in speed, utility and usability. *BMC*
549 *Bioinformatics* **22**, 433 (2021).

550 34. Bass, G. T. *et al.* Automated image analysis identifies signaling pathways regulating distinct
551 signatures of cardiac myocyte hypertrophy. *J. Mol. Cell. Cardiol.* **52**, 923–930 (2012).
552 35. Sarangdhar, M. *et al.* Data mining differential clinical outcomes associated with drug regimens
553 using adverse event reporting data. *Nat. Biotechnol.* **34**, 697–700 (2016).
554 36. Yap, T. A. *et al.* First-in-Human Phase I Trial of Two Schedules of OSI-930, a Novel Multikinase
555 Inhibitor, Incorporating Translational Proof-of-Mechanism Studies. *Clin. Cancer Res. Off. J. Am. Assoc.*
556 *Cancer Res.* **19**, 10.1158/1078-0432.CCR-12–2258 (2013).
557 37. Chan, S. H. Y., Khatib, Y., Webley, S., Layton, D. & Salek, S. Identification of cardiotoxicity related
558 to non-small cell lung cancer (NSCLC) treatments: A systematic review. *Front. Pharmacol.* **14**,
559 1137983 (2023).
560 38. Xu, Z. *et al.* Inhibition of PRKAA/AMPK (Ser485/491) phosphorylation by crizotinib induces
561 cardiotoxicity via perturbing autophagosome-lysosome fusion. *Autophagy* **20**, 416–436.
562 39. Kasper, S. *et al.* Differences in the dynamics of serotonin reuptake transporter occupancy may
563 explain superior clinical efficacy of escitalopram versus citalopram. *Int. Clin. Psychopharmacol.* **24**,
564 119–125 (2009).
565 40. Sanchez, C., Reines, E. H. & Montgomery, S. A. A comparative review of escitalopram,
566 paroxetine, and sertraline: are they all alike? *Int. Clin. Psychopharmacol.* **29**, 185 (2014).
567 41. Kasner, M. T. *et al.* A phase Ib dose escalation study of oral monotherapy with KX2-391 in elderly
568 patients with acute myeloid leukemia. *Invest. New Drugs* **40**, 773–781 (2022).
569 42. Crabol, Y., Catherinot, E., Veziris, N., Jullien, V. & Lortholary, O. Rifabutin: where do we stand in
570 2016? *J. Antimicrob. Chemother.* **71**, 1759–1771 (2016).
571 43. Pivonello, R., De Leo, M., Cozzolino, A. & Colao, A. The Treatment of Cushing's Disease. *Endocr.*
572 *Rev.* **36**, 385–486 (2015).

573 44. Hajialyani, M. *et al.* Hesperidin as a Neuroprotective Agent: A Review of Animal and Clinical
574 Evidence. *Mol. Basel Switz.* **24**, 648 (2019).
575 45. Thase, M. E., Larsen, K. G., Reines, E. & Kennedy, S. H. The cardiovascular safety profile of
576 escitalopram. *Eur. Neuropsychopharmacol. J. Eur. Coll. Neuropsychopharmacol.* **23**, 1391–1400
577 (2013).
578 46. Kimura, K. *et al.* Cardiovascular adverse reactions associated with escitalopram in patients with
579 underlying cardiovascular diseases: a systematic review and meta-analysis. *Front. Psychiatry* **14**,
580 1248397 (2023).
581 47. Heppt, M. V. *et al.* Comparative Efficacy and Safety of Tirbanibulin for Actinic Keratosis of the
582 Face and Scalp in Europe: A Systematic Review and Network Meta-Analysis of Randomized Controlled
583 Trials. *J. Clin. Med.* **11**, 1654 (2022).
584 48. Darpo, B., Bullingham, R., Combs, D. L., Ferber, G. & Hafez, K. Assessment of the cardiac safety
585 and pharmacokinetics of a short course, twice daily dose of orally-administered mifepristone in
586 healthy male subjects. *Cardiol. J.* **20**, 152–160 (2013).
587 49. Mathew, S., Ticsa, M. S., Qadir, S., Rezene, A. & Khanna, D. Multiple Clinical Indications of
588 Mifepristone: A Systematic Review. *Cureus* **15**, e48372.
589 50. Phillips, M. C., Wald-Dickler, N., Loomis, K., Luna, B. M. & Spellberg, B. Pharmacology, Dosing,
590 and Side Effects of Rifabutin as a Possible Therapy for Antibiotic-Resistant Acinetobacter Infections.
591 *Open Forum Infect. Dis.* **7**, ofaa460 (2020).
592 51. Ikeda, K. *et al.* The effects of sarpogrelate on cardiomyocyte hypertrophy. *Life Sci.* **67**, 2991–
593 2996 (2000).
594 52. Shimizu, K. *et al.* The Selective Serotonin 2A Receptor Antagonist Sarpogrelate Prevents Cardiac
595 Hypertrophy and Systolic Dysfunction via Inhibition of the ERK1/2–GATA4 Signaling Pathway.
596 *Pharmaceuticals* **14**, 1268 (2021).

597 53. Vadas, O. *et al.* Molecular determinants of PI3Kγ-mediated activation downstream of G-protein–
598 coupled receptors (GPCRs). *Proc. Natl. Acad. Sci.* **110**, 18862–18867 (2013).
599 54. Aghajanian, H. *et al.* Targeting Cardiac Fibrosis with Engineered T cells. *Nature* **573**, 430–433
600 (2019).
601 55. Palandri, C. *et al.* Pharmacological Management of Hypertrophic Cardiomyopathy: From Bench
602 to Bedside. *Drugs* **82**, 889–912 (2022).
603 56. Sapna, F. *et al.* Advancements in Heart Failure Management: A Comprehensive Narrative Review
604 of Emerging Therapies. *Cureus* **15**, e46486.
605 57. Abdelsayed, M., Kort, E. J., Jovinge, S. & Mercola, M. Repurposing drugs to treat cardiovascular
606 disease in the era of precision medicine. *Nat. Rev. Cardiol.* **19**, 751–764 (2022).
607 58. Kirouac, D. *et al.* Creating and analyzing pathway and protein interaction compendia for
608 modelling signal transduction networks. *BMC Syst. Biol.* **6**, 29 (2012).
609 59. Chen, B., Fan, W., Liu, J. & Wu, F.-X. Identifying protein complexes and functional modules--from
610 static PPI networks to dynamic PPI networks. *Brief. Bioinform.* **15**, 177–194 (2014).
611 60. Kabir, M. H., Patrick, R., Ho, J. W. K. & O'Connor, M. D. Identification of active signaling
612 pathways by integrating gene expression and protein interaction data. *BMC Syst. Biol.* **12**, 120 (2018).
613 61. Liu, A. *et al.* From expression footprints to causal pathways: contextualizing large signaling
614 networks with CARNIVAL. *NPJ Syst. Biol. Appl.* **5**, 40 (2019).
615 62. Frank, D. U., Sutcliffe, M. D. & Saucerman, J. J. Network-based predictions of in vivo cardiac
616 hypertrophy. *J. Mol. Cell. Cardiol.* **121**, 180–189 (2018).
617 63. Ahmed, L. A., Shiha, N. A. & Attia, A. S. Escitalopram Ameliorates Cardiomyopathy in Type 2
618 Diabetic Rats via Modulation of Receptor for Advanced Glycation End Products and Its Downstream
619 Signaling Cascades. *Front. Pharmacol.* **11**, 579206 (2020).

620 64. Bush, E. *et al.* A small molecular activator of cardiac hypertrophy uncovered in a chemical screen
621 for modifiers of the calcineurin signaling pathway. *Proc. Natl. Acad. Sci. U. S. A.* **101**, 2870–2875
622 (2004).
623 65. Mialet-Perez, J. *et al.* Serotonin 5-HT2A receptor-mediated hypertrophy is negatively regulated
624 by caveolin-3 in cardiomyoblasts and neonatal cardiomyocytes. *J. Mol. Cell. Cardiol.* **52**, 502–510
625 (2012).
626 66. Gao, W. *et al.* HTR2A promotes the development of cardiac hypertrophy by activating PI3K-
627 PDK1-AKT-mTOR signaling. *Cell Stress Chaperones* **25**, 899–908 (2020).
628 67. Schumacher, S. M. *et al.* Paroxetine-mediated GRK2 inhibition reverses cardiac dysfunction and
629 remodeling after myocardial infarction. *Sci. Transl. Med.* **7**, 277ra31 (2015).
630 68. Thal, D. M. *et al.* Paroxetine is a direct inhibitor of g protein-coupled receptor kinase 2 and
631 increases myocardial contractility. *ACS Chem. Biol.* **7**, 1830–1839 (2012).
632 69. Sun, X. *et al.* Paroxetine Attenuates Cardiac Hypertrophy Via Blocking GRK2 and ADRB1
633 Interaction in Hypertension. *J. Am. Heart Assoc. Cardiovasc. Cerebrovasc. Dis.* **10**, e016364 (2020).
634 70. Bouley, R. *et al.* Structural Determinants Influencing the Potency and Selectivity of Indazole-
635 Paroxetine Hybrid G Protein-Coupled Receptor Kinase 2 Inhibitors. *Mol. Pharmacol.* **92**, 707–717
636 (2017).
637 71. Ferrero, K. M. & Koch, W. J. GRK2 in cardiovascular disease and its potential as a therapeutic
638 target. *J. Mol. Cell. Cardiol.* **172**, 14–23 (2022).
639 72. Ren, R., Oakley, R. H., Cruz-Topete, D. & Cidlowski, J. A. Dual Role for Glucocorticoids in
640 Cardiomyocyte Hypertrophy and Apoptosis. *Endocrinology* **153**, 5346–5360 (2012).
641 73. Severinova, E. *et al.* Glucocorticoid Receptor-Binding and Transcriptome Signature in
642 Cardiomyocytes. *J. Am. Heart Assoc.* **8**, e011484 (2019).

643 74. Oakley, R. H. *et al.* Essential role of stress hormone signaling in cardiomyocytes for the
644 prevention of heart disease. *Proc. Natl. Acad. Sci. U. S. A.* **110**, 17035–17040 (2013).
645 75. Pianca, N. *et al.* Glucocorticoid receptor antagonization propels endogenous cardiomyocyte
646 proliferation and cardiac regeneration. *Nat. Cardiovasc. Res.* **1**, 617–633 (2022).
647 76. Ping, P. *et al.* Formation of protein kinase Cε-Lck signaling modules confers cardioprotection. *J.*
648 *Clin. Invest.* **109**, 499–507 (2002).
649 77. Zou, J. *et al.* C/EBPβ knockdown protects cardiomyocytes from hypertrophy via inhibition of
650 p65-NFκB. *Mol. Cell. Endocrinol.* **390**, 18–25 (2014).
651 78. Redondo-Angulo, I. *et al.* C/EBPβ is required in pregnancy-induced cardiac hypertrophy. *Int. J.*
652 *Cardiol.* **202**, 819–828 (2016).
653
654

655 **Supplemental Figures**

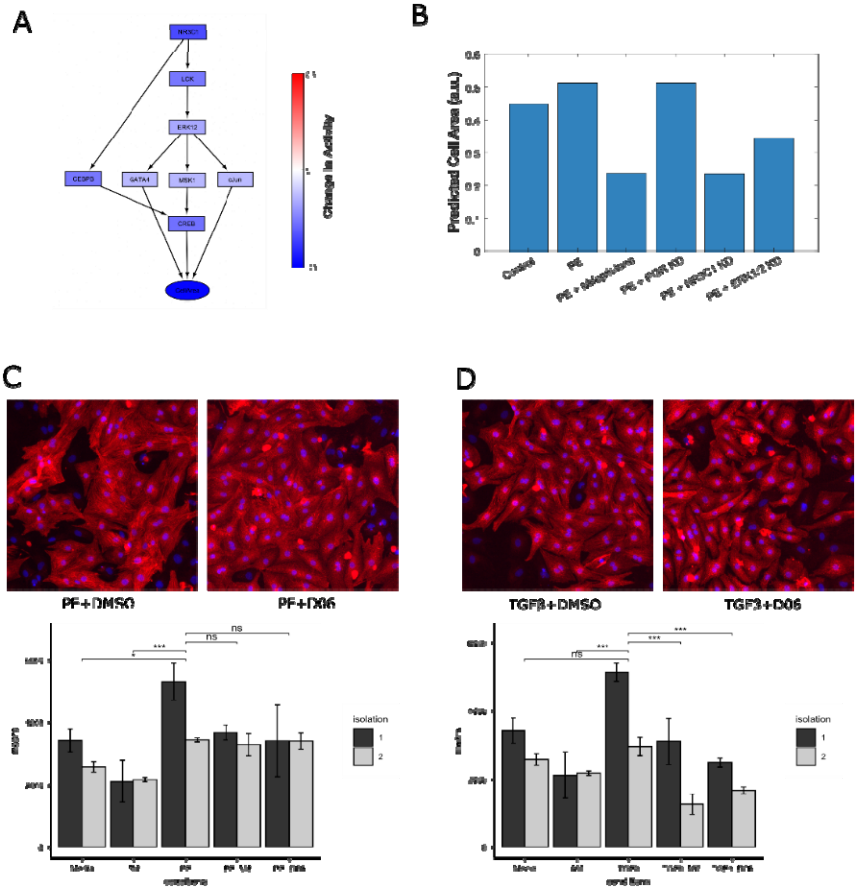

656

657 **Supplemental Figure 1. Mifepristone prevents cardiomyocyte hypertrophy through glucocorticoid**

658 **receptor inhibition.** A) Mechanistic subnetwork analysis predicts that mifepristone suppresses

659 cardiomyocyte hypertrophy through the glucocorticoid receptor via LCK and CEBPβ. Prior studies have

660 shown that the glucocorticoids and the glucocorticoid receptor may be either hypertrophic or

661 antihypertrophic[72], and it is not clear what mechanisms control these divergent effects. The role of LCK

662 has not been described in hypertrophy, however it is known to mediate cardioprotection from ischemic

663 injury[76]. B) Simulations of PE-induced hypertrophy and modulation by mifepristone, progesterone

664 inhibition, glucocorticoid receptor inhibition, or ERK ½ inhibition. Glucocorticoid receptor inhibition by

665 AL082D06 (20 μM) significantly prevents C) PE- and D) TGFβ-induced cardiomyocyte hypertrophy 48

666 hours post treatment, as shown by representative images and quantification of automated

667 segmentation. CEBPβ has been previously been shown to regulate cardiac hypertrophy[77,78].

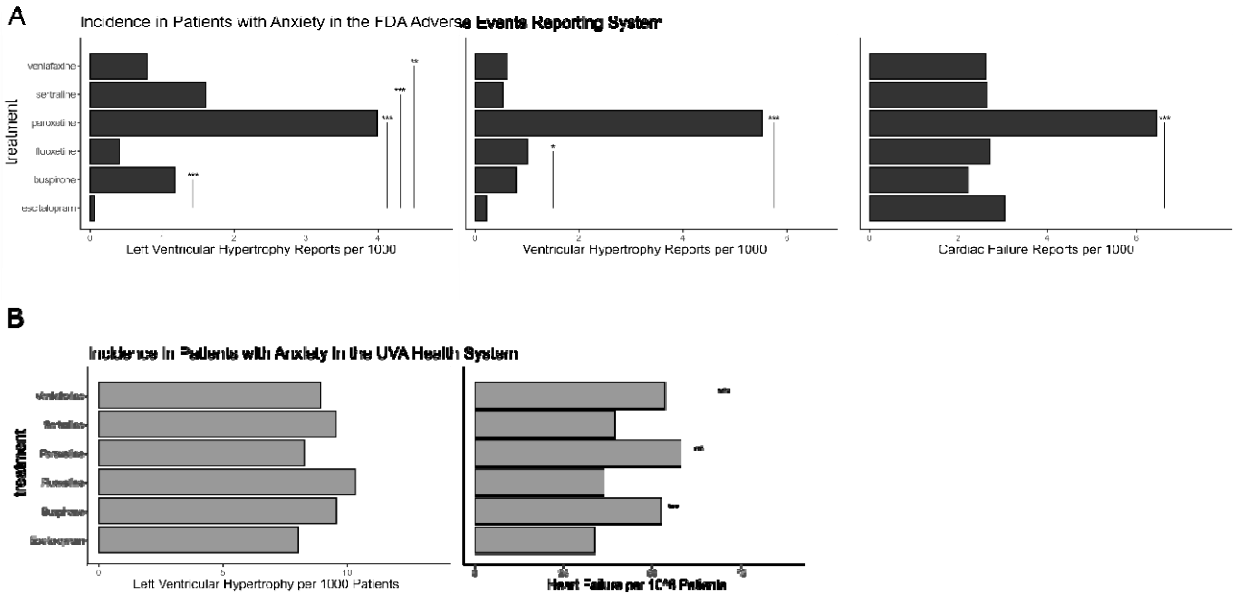

668

669

670 **Supplemental Figure 2. Left ventricular hypertrophy is less frequently reported among anxiety**

671 **patients taking escitalopram.** A) Reports of left ventricular hypertrophy (left), ventricular hypertrophy

672 (center), or cardiac failure (right) per 1000 patients are shown for anxiety patients taking either

673 escitalopram or another anxiolytic (buspirone, fluoxetine, paroxetine, sertraline or venlafaxine). B)

674 Diagnoses of left ventricular hypertrophy per 1000 (left) or heart failure per 1 million (right) patients are

675 shown for anxiety patients taking either escitalopram or another anxiolytic.